American Mineralogist, Volume 80, pages 1293–1301, 1995

The fate of olivine in subducting slabs: A reconnaissance study

P. C. BURNLEY*

Center for High Pressure Research and Department of Geological and Geophysical Sciences, Princeton University, Princeton, New Jersey 08544, U.S.A.

ABSTRACT

To explore the transformation behavior of metastable olivine at large overpressures equivalent to 500–670 km depth, a reconnaissance study using Mg_2GeO_4 olivine at pressures up to 16 GPa was conducted. Optical microscopy and transmission electron microscopy of the specimens were used to observe the behavior of both the reconstructive and martensitic-like transformation mechanisms. The experiments revealed that the kinetics of the thermally activated reconstructive transformation are insensitive to pressure; comparison with previous growth rate measurements made at 1–2 GPa lead to an estimate of the activation volume for growth of $V^* = 0 \pm 2$ cm³/mol. In contrast, the martensitic-like mechanism becomes more important at high pressure, producing optically visible features in Mg_2GeO_4 olivine by 9 GPa. Similar conditions would be experienced by natural olivine that has metastably persisted in cold subducting slabs to the bottom of the transition zone, these observations suggest that the conversion of natural olivine to its spinel structure by the martensitic-like mechanism could become significant in that environment. This conversion would provide a uniform final cut-off depth for earthquakes caused by transformational faulting independent of slab thermal structure.

INTRODUCTION

There is both experimental (Sung and Burns, 1976; Sung, 1979; Burnley and Green, 1989; Green and Burnley, 1989; Rubie et al., 1990; Burnley et al., 1991, 1995; Wu et al., 1993; Rubie and Ross, 1994) and seismic (Iidaka and Suetsugu, 1992) evidence to suggest that olivine, the primary constituent of the upper mantle, may persist metastably within cold subducting lithospheric slabs to great depths. Transformation to the spinel-structure polymorph (γ) proceeds by a thermally activated reconstructive mechanism over a large range of depths when the temperature becomes sufficiently high (Sung and Burns, 1976; Green and Burnley, 1989; Kirby et al., 1991; Rubie and Ross, 1994). Therefore, knowledge of the effect of pressure on transformation rate is important for extrapolating measured transformation kinetics to the environment in subducting slabs. Unfortunately, reconstructive transformation kinetics generally have been studied over only a narrow pressure range relatively close to the equilibrium phase boundary for any given olivine composition (Burnley, 1990; Rubie et al., 1990). Ungasketed diamond-anvil cell (DAC) experiments often cover the entire range of transformation zone pressures within a single sample (Sung, 1979; Wu et al., 1993; Burnley et al., 1995), but the extreme levels of shear stress and plastic strain as well as small sample size make interpretation difficult and the measurement of hydrostatic transformation kinetics impossible. Because martensitic-like (ML) transformation had never been observed to produce more than nanoscale transformation ($\ll 0.1\%$), no study of the kinetics of this mechanism had ever been conducted.

To study transformation kinetics over a wide range of pressures far from equilibrium, reconnaissance experiments were conducted using Mg_2GeO_4, which has both an olivine (α) and a spinel (γ) structure. Although it is commonly done, it is not strictly correct to refer to these phases as "olivine" and "spinel" because these are mineral names. In this paper the designations α and γ are used to refer to the olivine and spinel-structure phases for all chemistries other than the natural silicate. The germanate olivine analog (α) is ideal for studying transformation kinetics as a function of pressure because (1) the transformation kinetics have been well characterized near the equilibrium phase boundary, and quantitative measurements of grain growth rates have been made under those conditions (Burnley, 1990), and (2) conditions ranging across the entire spinel-phase (γ) field can be accessed for a relatively large sample size ($\sim 3 \times 3$ mm) using the multi-anvil press. The sample size, which is large relative to the grain size, allows petrographic observations to be made over large regions and permits differentiation between behavior associated with sample edges and that associated with the bulk. The absence of two-phase fields and the intermediate β phase in this analog are not a problem for a study of this type because below approximately 400 km depth, the transition in the slab

* Present address: Cooperative Institute for Research in Environmental Sciences, Campus Box 216, University of Colorado, Boulder, Colorado 80309-0216, U.S.A.

0003–004X/95/1112–1293$02.00

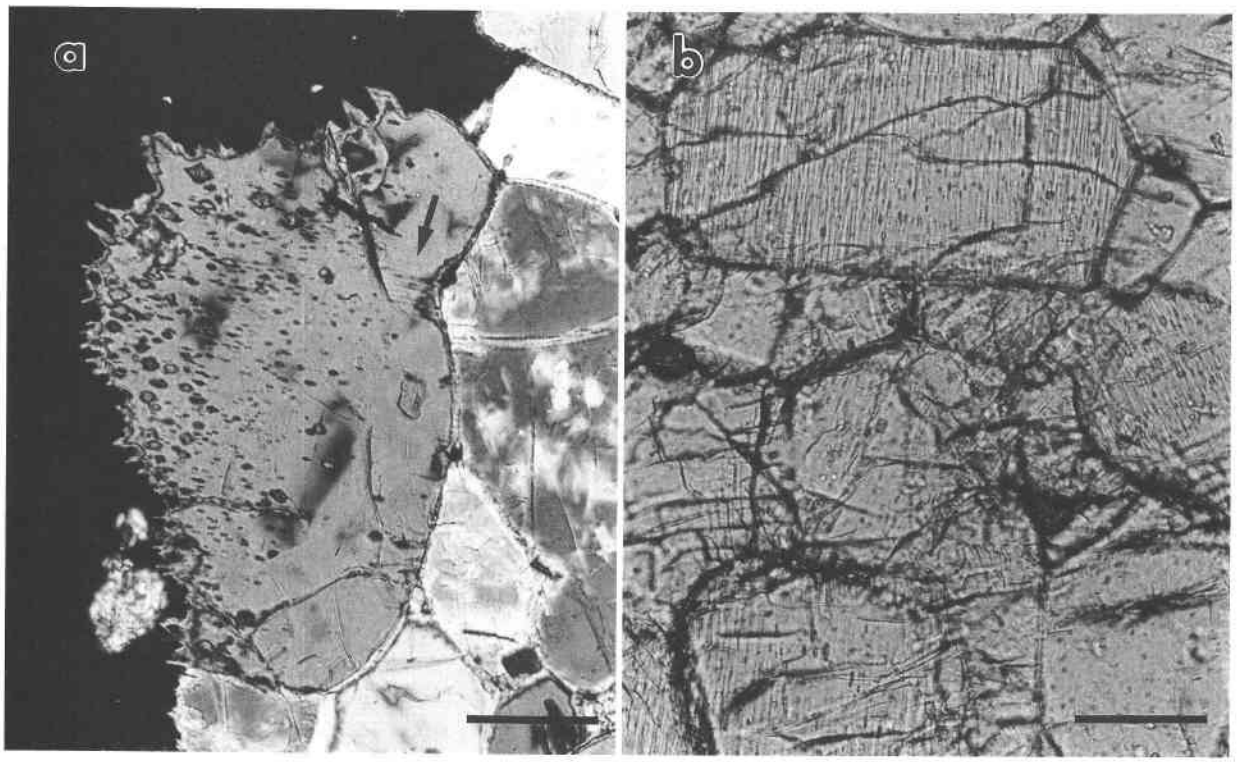

Fig. 1. (**a**) Photomicrograph of sample 1784 (9 GPa, 990 °C, 10 min). Fingers of γ form a rind growing on Pt capsule wall (extreme left). Small amounts of γ are also present on α grain boundaries (upper right). The γ is black between crossed polars, but where it overlaps with α the result is a reduction of birefringence. Small inclusions within a large α grain appear to be γ grains nucleated on martensitic lamellae that cut the grain horizontally and are most visible along the upper right side of the grain (arrow). Scale bar is 50 μm. (**b**) Photomicrograph of 1792 (15.5 GPa, 1000 °C, 10 min) in plane-polarized light. Most α grains in specimen exhibit striations similar to those seen here. Optical evidence of martensitic-like transformation has never been seen before. Several grains in the specimen retrieved from 990 °C and 9 GPa also contained these striations, but none were observed in the sample that was pressurized to 16 GPa but was not heated. Scale bar is 50 μm.

is isochemical and directly from olivine to γ (Akaogi et al., 1989; Kirby et al., 1991).

The experiments were conducted in the 2000 ton split-sphere apparatus at the State University of New York at Stony Brook using the 14 mm octahedral MgO cell assembly with a graphite furnace (Gwanmesia and Liebermann, 1992) and Kennametal K313 WC cubes with 8 mm truncations. The sintered Mg_2GeO_4 α polycrystals had an average grain size of about 80 μm (Vaughan and Coe, 1981) and were contained in folded platinum capsules. Samples were pressurized at room temperature over a period ranging from 6 to 10 h and then heated to the final temperature in 15 min. A pressure calibration curve for the cell was constructed using the equilibria between quartz-coesite (1600 °C), $CaGeO_3$ (1000 °C), coesite-stishovite (1200 and 2000 °C) and α-β forsterite (1200 °C), as well as the information that the β-γ transition in forsterite could not be achieved using this cell (K. Leinenweber, personal communication). Temperature was either (1) measured using a W3%Re vs. W25%Re thermocouple with the junction formed on the capsule surface to ensure that the temperature measured was that of the sample or (2) determined from the power consumed by the furnace, which was calibrated in seven other experiments with identical furnace assemblies that contained a thermocouple. The W-Re wires were calibrated at room pressure and yielded an estimate of the total uncertainty associated with the use of the wire of ± 5 °C. This, plus the observed temperature-control variations and an estimate of error resulting from temperature gradients are included in the given uncertainty. An estimate of the effect of pressure on the electromotive force (emf) is not included in the uncertainty. The experiments were quenched by turning off the power to the furnace; the temperature returned to below 350 °C within 1 s. Decompression occurred overnight. Experimental products were examined using a light microscope, an ISI-SX30 scanning electron microscope (SEM) operating at 30 kV, and a JEOL 200-CX transmission electron microscope (TEM) operating at 200 kV. SEM samples were prepared by polishing and etching in HCl for one-half hour and then sputter coating with Au. TEM specimens

were thinned using a Gatan Ar ion mill and coated with amorphous carbon.

Results

Three experiments were conducted. In the first, in which there was no thermocouple, the sample was heated to 990 ± 60 °C at 9 ± 0.5 GPa for 600 s. It produced a 50–75 μm deep rind of γ on the platinum capsule wall. Small grains of γ (~5 μm) were also found on α grain boundaries. The γ on the grain boundaries and on the platinum wall exhibits typical reconstructive textures; forming fingers that grow into the α from the grain margins (Fig. 1a).

The second experiment, which contained two thermocouples, one on each end of the sample capsule, was conducted at 15.5 ± 1 GPa, and the sample was heated for 600 s. The measured temperatures were 1000 ± 10 °C and 948 ± 12 °C. This sample contained γ nucleated on the capsule margin, along one side and across both ends of the capsule adjacent to the thermocouples. The γ rind was 40 μm deep along the hotter end of the sample and 20 μm deep along the colder end. Small γ grains were also observed on α-α grain boundaries within 750 μm of the sample edge. Nearly all the α grains within the specimen contained very fine striations (Figs. 1b and 2). Upon further examination, several α grains within the 9 GPa experiment were also found to contain small regions with striations (see arrow in Fig. 1a). TEM shows that these striations are ML lamellae of γ (Fig. 3a). The selected-area diffraction pattern (Fig. 3b) confirms the presence of γ within the lamellae and contains the characteristic streaking along $(100)_\alpha$ seen in other studies (Lacam et al., 1980; Boland and Liu, 1983; Burnley and Green, 1989; Madon et al., 1989). From the TEM images it appears that as much as 10% of individual α grains transformed to γ by the ML mechanism. In TEM images, lamellae are typically observed to be 14 nm wide but can be as large as 120 nm wide. SEM images reveal some grain-to-grain variation in lamellar width; lamellae as wide as 280 nm were identified. Lamellae can span entire grains but some are only a few micrometers long.

In the third experiment, a sample was pressurized to 15.5 ± 1 GPa but not heated, remaining at 22 ± 5 °C. No γ was observed in this specimen, and no striations were visible.

Fig. 2. Scanning electron micrograph of polished and etched surface of sample 1792 (15.5 GPa, 1000 °C). The α etches more rapidly than γ, leaving γ standing in relief. The three-dimensional nature of the lamellae can be seen because individual lamellae are exposed on both the polished surface and the inner surfaces of cracks. Large cracks contain some epoxy (smooth, slightly darker material). Scale bar is 2 μm.

Discussion

Transformation kinetics are thought to be governed by the rates at which two phenomena occur: nucleation and growth. These experiments provide information about how pressure affects the rates of both of these processes for the reconstructive transformation. In addition, new insight was gained into the operation of the ML mechanism and its geologic importance.

Reconstructive kinetics

Growth rates for Mg_2GeO_4 γ growing in α have been well characterized at pressures close to the equilibrium boundary (Burnley, 1990). These growth rates can be compared with those estimated from the 16 GPa experiment in which temperature was measured and an estimate of the pressure dependence of the activation energy (V^*) can be obtained. Grain-boundary velocities have been determined at 1 and 2 GPa by measuring the sizes of isolated, reconstructively coarsened, martensitically nucleated grains (Table 1) (Burnley, 1990). In the 16 GPa experiment nucleation times for γ grains are not known. However, Burnley (1990) found that the depth of rinds observed on the platinum capsules at 1 and 2 GPa were consistent with instantaneous nucleation on the platinum wall. Therefore, if it is assumed that nucleation was instantaneous on the platinum surface and that all the thickness of the rind can be attributed to growth of γ grains from the platinum capsule into the α, then an estimate of the growth rate can be obtained. The first assumption is the most difficult to justify and will be discussed later. The second assumption should lead to only a small overestimate of growth rates because (1) nuclei should be well under a micrometer in size, and (2) the rinds are only a few grains deep, and each grain appears to have nucleated on the surface of the γ-α interface and grown into the α. The critical nucleus varies inversely with the free energy released by transformation (Christian, 1975). Grains well under a half micrometer in size have been observed by the author under conditions close

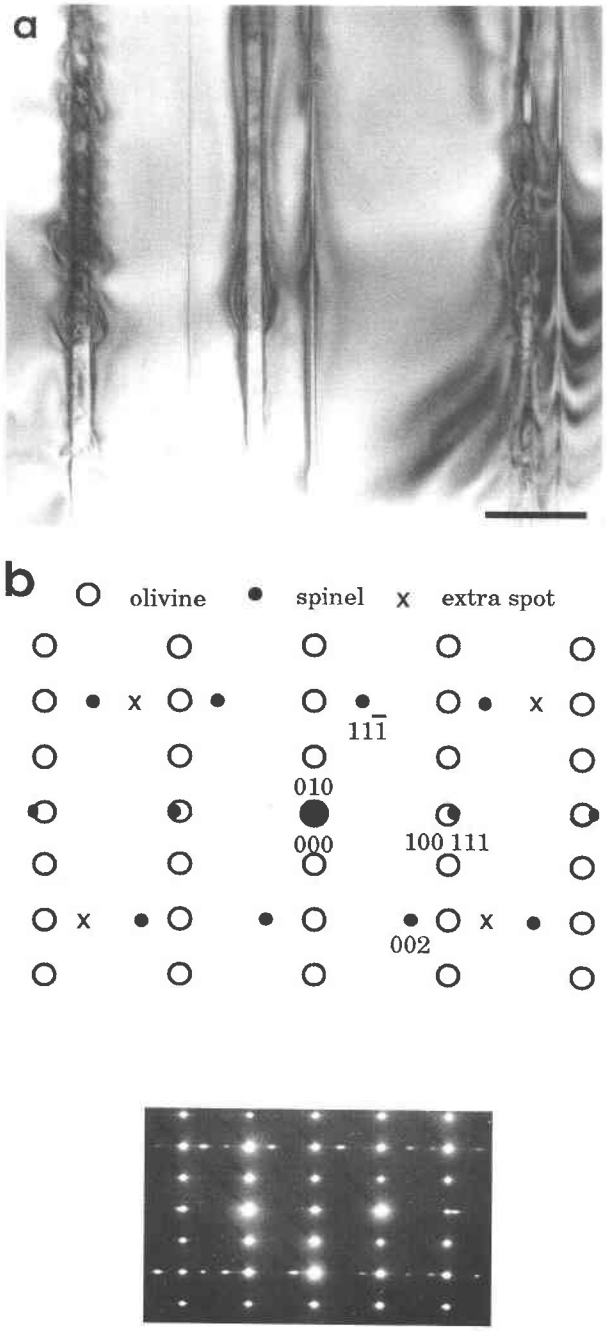

Fig. 3. (**a**) Transmission electron micrograph of γ lamellae in α (sample 1792, 15.5 GPa, 1000 °C, 10 min). Strain contrast because of misfit between α and γ lattices can be seen along the edges of the lamellae. Scale bar is 0.25 μm. (**b**) Selected-area diffraction pattern (taken from region shown in **a**) showing superposition of [001] α zone and [$\bar{1}$10] γ zone. This orientation relationship between γ lamellae and their α host has been predicted (Poirier, 1981) and previously observed (Boland and Liu, 1983; Burnley and Green, 1989; Madon et al., 1989). Key shows indexing of patterns and the location of extra spots, which result from either double diffraction or twinning in the γ (Brearley and Burnley, in preparation).

Table 1. Growth rate data

Sample*	P (GPa)	T (K)	$\dot{x} \times 10^{-9}$ (m/s)
GL312	1.09	1181(14)	3.23(0.6)
GL307	1.45	1204(10)	5.67(0.6)
GL307	1.45	1172(11)	2.83(0.3)
GL299	1.19	1210(11)	4.37(0.9)
GL313	1.89	1205(14)	5.95(1.2)
GL313	1.89	1171(10)	1.59(0.3)
GL326	1.92	1284(15)	30.5(6.2)
GL326	1.92	1299(11)	66.7(13)
1792	15.5	1273(10)	66.6(13)
1792	15.5	1221(12)	33.3(6.7)

* Sample names beginning with GL are from Burnley (1990).

to the equilibrium boundary where the free energy release is considerably smaller. Therefore, neglecting the volume resulting from nucleation contributes only a small amount to the uncertainty.

In the 16 GPa experiment two thermocouples were present, one at either end of the sample capsule; the temperatures varied by 50 °C. The depth of the rind was measured at each end. Growth rates derived from these measurements (Table 1) are plotted along with data gathered at 1–2 GPa by Burnley (1990). The equation that describes interface-controlled growth is written as

$$\ln \dot{x} = \ln K_0 + \ln T + \frac{-H^*}{RT} + \frac{-PV^*}{RT} + \ln\left[1 - \exp\left(\frac{\Delta G}{RT}\right)\right]$$

where $\dot{x}$ is the rate at which the boundary between the phases advances, K_0 is a constant, H^* is activation enthalpy, V^* is activation volume, ΔG is the free-energy difference between the two phases, R is the gas constant, and P and T are pressure and temperature, respectively. The free energy change for each pressure-temperature condition, under which data were gathered, was estimated using thermodynamic data given in Ross and Navrotsky (1987). Best-fit values for V^*, ln K_0, and H^* were determined using a nonlinear least-squares fit using a Levenberg-Marquardt algorithm. Several fits were made, and values for the fit parameters are given in Table 2. The numerical fitting process was not particularly well conditioned, showing some degree of linear dependence. However, the solutions are consistent with a by-eye fit and exhibit the basic features that are obvious from Figure 4: The pressure dependence must be quite small to fit the entire data set. Fitting the entire data set yielded a surface that did not fit the 1 and 2 GPa data as well as fits that broke the data into two sections. The fit for the 1–2 GPa data yielded a V^* of 9 ± 3 cm^3/mol, whereas the fit to the 2 and 16 GPa data yielded a V^* of −0.2 ± 0.2 cm^3/mol. Therefore, the poor fit yielded for the whole data set may be due to forcing V^* to be constant with pressure. The fit to the 1–2 GPa data shows a high degree of linear dependence, indicating that the model is over parameterized; this is because of the small spread in pres-

TABLE 2. Modeling results

	ln K_0	H^*	V^*
All data	5(3)	3.0(0.3) × 10^5	−0.1(0.2)
1–2 GPa data	9(3)	3.3(0.3) × 10^5	9(3)
2 and 16 GPa data	9(3)	3.5(0.3) × 10^5	−0.2(0.2)
−100° shift	6(3)	3.1(0.3) × 10^5	1.7(0.3)
+100° shift	4(4)	2.9(0.4) × 10^5	−1.9(0.3)

Note: The asymptotic standard error is given in parentheses.

sure of the data points. Therefore, although the value of 9 cm³/mol for V^* is consistent with the value obtained by others at these pressures (Rubie and Ross, 1994), this value for V^* should be used with caution. Another possible difficulty with treating the 1–2 and the 16 GPa data as a single data set is that different types of thermocouples were used in the experiments and the effect of pressure on emf was not taken into account. Although it is thought to be small, the effect of pressure on the W3%Re vs. W25%Re thermocouples is not known. To test for the effect of a relative shift in temperature scales between the two experimental data sets, fits were made to a data set in which the temperature of the 16 GPa data was shifted 100° up and down. These fits yielded V^* values of -1.9 ± 0.3 and 1.7 ± 0.2, respectively. These values differ from those obtained by assuming an uncertainty of ±100° for these data in that the temperatures for the two 16 GPa data points are shifted together. One of the reasons that such large offsets in temperature do not yield a more dramatic difference in the fit parameters is that the slope defined by the high-pressure data points remains the same. Figure 4 shows a combination of model surfaces. Below 2 GPa fit parameters for the low-pressure data are used. Above 2 GPa the fit made using the 2 and 16 GPa data is plotted. The surface at 2 GPa is identical for both models. The intersection of the model surface with 16 GPa is also shown for the models fit for the temperature-shifted data. Taking into account the uncertainty associated with the assumptions discussed above, the best estimate of V^* is 0 ± 2 cm³/mol. If nucleation on the platinum margin is not instantaneous then the growth rates in the 16 GPa experiment are underestimates (by an amount that is a function of the incubation period). This would have the effect of forcing V^* to become negative.

The information about nucleation rates gained from these experiments is more qualitative, but it is also consistent with a pressure insensitivity. Typically in hydrostatic experiments conducted closer to the equilibrium phase boundary, γ begins to nucleate and grow on the platinum capsule-sample interface first and only later on interior α-α grain boundaries (Rubie and Champness, 1987; Burnley, 1990). This growth pattern was also observed in the experiments described here. These observations argue that the process of nucleating γ in α is not dramatically affected by pressure once the immediate vicinity of the equilibrium boundary is exceeded. This is in agreement with the prediction of the theory of heterogeneous nucleation if V^* is small.

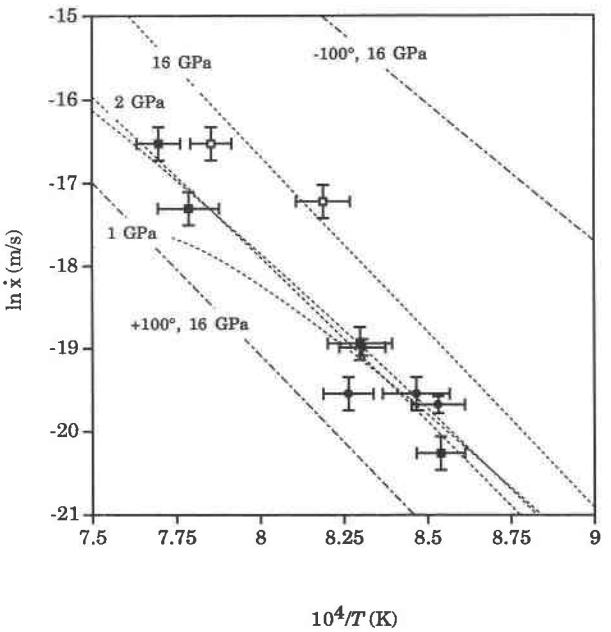

Fig. 4. Natural log of grain growth data plotted vs. $1/T$. Solid symbols are for data collected between 1 and 2 GPa from Burnley (1990). Open squares are for growth rates estimated from 16 GPa experiment. Dashed lines represent position of fit surfaces at 1, 1.5, 2, and 16 GPa. Position of fit surface at 16 GPa for temperature-shifted data are shown with dot-dashed lines. The 1 and 1.5 GPa lines are for fit surfaces at 1–2 GPa data. The 16 GPa line is for fit surface at 2 and 16 GPa data. Fit surface at 2 GPa data is identical for both models. Fit parameters are given in Table 2.

This insensitivity of reconstructive transformation kinetics to changes in pressure is consistent with patterns observed in DAC experiments (Sung, 1979; Burnley et al., 1995). Thus, it is reasonable to estimate transformation rates throughout the subducting slab on the basis of kinetics laws derived from transformation experiments made over a limited range of pressures.

Martensitic-like kinetics

Poirier (1981) proposed that the O lattice of the γ phase can form coherently from α by the propagation of partial dislocations on the (100) plane of α. The cations must reach their positions by synchroshear, or, alternatively, they may remain in their α configurations and become ordered in the γ-structure sites only after short-range diffusion (Wu et al., 1993; Furnish and Bassett, 1983). This mechanism is referred to as martensitic-like (ML) because it is unlike true martensitic transformation in which all the atoms reach their sites by means of the same crystallographic operation. Microstructural evidence that indicates the operation of the mechanism includes narrow lamellae of the γ phase lying parallel to (100) in α with the topotactic relationship (100)α parallel to (111)γ, [001]α parallel to [$\bar{1}$10]γ. In previous studies, ML transformation had never been observed to produce optically visible

quantities of the γ phase in α. Lamellae of the γ phase are typically no more than several unit cells thick (Burnley and Green, 1989), and experimental observations have always used TEM (Lacam et al., 1980; Boland and Liu, 1983; Burnley and Green, 1989; Burnley et al., 1995). Even in DAC experiments it has been shown that reconstructive transformation accounts for much or all of the optically observable γ (Sung, 1979; Burnley et al., 1995). The question is, why is the extent of transformation by the ML mechanism so much larger in these experiments? The amount of transformation achieved by any mechanism depends to a varying extent upon the pressure, temperature, time, and differential stress as well as the microstructure of the starting material. Evidently, these experiments were conducted under conditions that had not been tested before.

Temperature. The observation that large lamellae did not form in the room temperature experiment indicates that thermal activation plays a role in ML kinetics. This is not surprising because the cations must move to new sites during or after shearing of the anion lattice; the glide of dislocations is also known to be thermally activated (Poirier, 1991). The lamellae could have formed during heating, therefore the exact temperature required to form them and details of the effect of temperature on ML kinetics need to be determined by further study.

Differential stress. In contrast to previous work, the ML lamellae in this study did not form in association with high differential stresses. At low pressure (1–2 GPa) approximately 1 GPa of differential stress is required to form γ-phase lamellae (Burnley, 1990). However, even in samples from ungasketed DAC experiments in which stress levels are very high, lamellae remain small (Burnley et al., 1995). The level of differential stress in the multi-anvil experiments presented here is unknown but may be as high as 1 GPa at room temperature (Liebermann and Wang, 1992). The stress within the cell decays as the assembly is heated and the MgO confining media relaxes. Therefore, the reconstructive growth observed in the experiments probably occurred when differential stress levels were quite low; this is confirmed by the lack of γ-phase lenses that invariably form when modest differential stresses are present (e.g., Burnley et al., 1991, 1995). TEM reveals relatively little deformation and very few dislocations in the host α, in marked contrast to other samples containing ML lamellae such as those from DAC experiments and the samples of Burnley and Green (1989), which contained high dislocation densities. Thus, although the stress associated with the formation of the lamellae cannot be exactly determined, we do know that the ML lamellae were produced under conditions where the yield strength of the α was not exceeded.

Sample microstructure. A significant difference between the samples examined in this study and other samples that contain ML lamellae is that the samples from this study are not significantly deformed. The transformation mechanism depends upon the glide of partial dislocations on the (100) plane of α. If these partial dislocations become hung up on other dislocations or subgrain boundaries, the lamellae may not be able to propagate across the entire crystal or grow more than one or two unit cells in thickness. Although other studies conducted under supposedly hydrostatic conditions started with undeformed materials, it is likely that the amount of plastic strain induced into samples to bring them to similar conditions is sufficient to make operation of the mechanism impossible. For example, in multi-anvil experiments, the sample assemblies required to reach silicate perovskite stability produce shock microstructures in the $(Mg,Fe)_2SiO_4$ olivine (α) during pressurization (Y. Wang, personal communication).

Pressure. The observation that more ML lamellae formed at 16 GPa than at 9 GPa suggests that increased pressure facilitates this transformation mechanism. The effect of pressure on ML transformation kinetics is twofold. First and foremost, it increases the free energy available to drive the transformation. Second, increasing pressure decreases the strain energy required to create ML lamellae. Because the lamellar interface is coherent, the strain energy owing to the lattice misfit between α and γ is a significant liability for the ML mechanism. However, α is more compressible than γ and becomes denser more rapidly with increasing pressure. Using the elastic moduli of Mg_2GeO_4 α and γ (Weidner and Hamaya, 1983), one predicts that although the ratio of the c axes remains approximately the same, the b axis of α becomes shorter than its parallel direction in γ at pressures > 12 GPa. Although this calculation is an approximation because of the lack of known pressure derivatives of the moduli for Mg_2GeO_4 α, it illustrates that the strain energy created by the formation of the lamellae should decrease with pressure. Combined with the increase in free energy driving the transformation, the decrease in strain energy should make ML transformation energetically favorable at a high-pressure overstep.

Although the experiments in this study do not demonstrate that complete transformation by the ML mechanism is possible, the observations do not suggest otherwise. The α remaining in between the lamellae does not contain many dislocations or other microstructures that might hinder further transformation. For metals, martensitic transformation occurs upon cooling, and the amount of martensitic transformation is often a function of temperature (i.e, degree of undercooling) rather than time. By analogy, as suggested by Rubie (1993), the amount of ML transformation in mineral systems in which volume change drives the transition should be a function of pressure rather than time. Therefore, it is reasonable to propose that higher degrees of transformation would have been achieved in the experiments if the pressure had exceeded 16 GPa. Figure 5 shows a schematic kinetic map to illustrate this concept. It is drawn for undeformed Mg_2GeO_4 under hydrostatic conditions and shows the location of the reconnaissance experiments for reference. ML start and finish curves are drawn as largely pressure dependent with some temperature dependence at very

low temperature, as indicated by the results from the reconnaissance experiments. The kinetic onset for reconstructive transformation to γ is shown as pressure independent except close to the equilibrium boundary, consistent with the observations of others (Sung, 1979; Rubie and Ross, 1994; Burnley et al., 1995) and those above. The kinetic onset of transformation to rock salt + ilmenite structure phases and the amorphization of α at high pressure and very low temperature are speculative but shown for completeness.

Application to natural compositions and the mantle

Mg_2GeO_4 is an analog system that has proved very useful for understanding certain aspects of the behavior of natural compositions of olivine (α) and its spinel-structure phase (γ). The γ phase was first discovered in the germanate analog. Mg_2GeO_4 participates in a continuous solid solution with Mg_2SiO_4 (Dachille and Roy, 1960; Ringwood, 1956) and differs only slightly in optical and physical properties; its elastic behavior is also very similar (Weidner and Hamaya, 1983). Transformation faulting and the development of anticracks were first observed in Mg_2GeO_4 (Green and Burnley, 1989; Burnley et al., 1991) and then confirmed in $(Mg,Fe)_2SiO_4$ (Green et al., 1990). However, the values of thermodynamic parameters and the position of the equilibrium boundary in pressure-temperature space do not carry from one system to the next, so observations made in the germanate system cannot be directly applied to the natural system. The most intuitively appealing and widely used method of transferring information from one system to another is to use the relative position on the phase diagram as a guide. At 16 GPa conditions are very close to the high-pressure decomposition reaction of Mg_2GeO_4 γ. Therefore, it is reasonable to expect that ML transformation in metastable natural olivine would increase close to the pressure-temperature conditions at which γ breaks down to perovskite + magnesiowüstite, and that reconstructive transformation rates would be relatively insensitive to increases in pressure across the γ field. Another method of extrapolation is suggested by the hypothesis that strain energy on the composition plane between α and γ should be minimized for ML transformation. The lattice spacings as a function of pressure for natural olivine and its γ phase have been estimated using compliances for Mg_2SiO_4 olivine from Kumazawa and Anderson (1969), first and second pressure derivatives estimated for $(Mg_{90.5}Fe_{9.5})SiO_4$ (Webb, 1989), and a Birch-Murnaghan equation of state for γ (Weidner et al., 1984; Rigden et al., 1991). Similar to the germanate, the misfit between the two lattices along the c direction of olivine remains constant while the misfit along the b direction decreases to zero at approximately 23 GPa. The misfit along the a direction reaches zero at 22 GPa. These pressures are in the vicinity of the γ decomposition reaction. In summary, the results from the Mg_2GeO_4 analog study suggest that reconstructive transformation rates for metastable natural olivine are pressure insensitive, and that at great depths metastable olivine begins to convert to the γ structure by the ML mechanism.

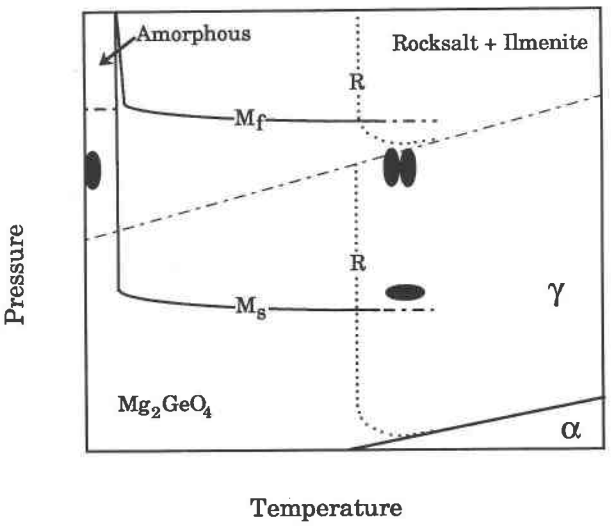

Fig. 5. Schematic kinetic map for undeformed Mg_2GeO_4 under hydrostatic conditions. Location of reconnaissance experiments shown as solid ovals. Solid lines M_s and M_f indicate ML start and finish curves for α to γ. Dotted lines R indicate the kinetic onset for reconstructive transformations α to γ and γ to rock salt + ilmenite structure phases. Equilibrium phase boundaries for α to γ (Ross and Navrotsky, 1987) (solid line) and γ to ilmenite + rock salt structure phases (Liu and Bassett, 1986) (dashed line) also shown.

These observations have interesting implications for the mantle. As discussed above, there is much evidence (including that presented here) to suggest that olivine can and does survive to the bottom of the transition zone in the core of cold subducting slabs. Recent experiments (Martinez et al., 1994) indicate that below 1000 K the sluggishness of the reconstructive transformation mechanism continues to at least 26 GPa (in this case the product phases should be perovskite + magnesiowüstite). If the reconstructive mechanism were the only transformation mechanism operating there would be nothing to stop olivine from being subducted into the lower mantle if the slab penetrates beyond 670 km. However, a model of subducting slabs could be constructed in which ML transformation rates increase within the slab at the bottom of the transition zone and complete what the reconstructive mechanism failed to do. An implication of such a model concerns deep earthquakes. It has been proposed that deep earthquakes are caused by transformation faulting (Kirby, 1987; Green and Burnley, 1989; Burnley et al., 1991; Kirby et al., 1991), which operates by means of reconstructive transformation (Burnley et al., 1991). Martensitic-like transformation would then "turn off" deep earthquakes when it eliminates the remaining olivine within the slab. Thus, deep earthquakes would not occur below the depth at which ML transformation is completed. This model would provide a uniform final cut-off for deep earthquakes that is independent of the

thermal structure of each subduction zone; this pattern is observed in the Earth. One final note concerning deep earthquakes. It has been proposed by several groups (Meade and Jeanloz, 1989; Lomnitz-Adler, 1990) that ML transformation could be the source of deep earthquakes. Although it now seems quite possible that ML transformation can occur in the Earth, it is still not clear how shear on the (100) planes of randomly oriented olivine grains could generate the large shear displacements inferred from observed double couple source mechanisms.

Conclusions

In conclusion, reconnaissance transformation experiments on metastable Mg_2GeO_4 α at 9 and 16 GPa indicate that reconstructive transformation rates are insensitive to pressure ($V^* = 0 \pm 2$ cm^3/mol) beyond the vicinity of the equilibrium phase boundary, but that the martensitic-like transformation rate increases at high overpressures. By analogy it is suggested that the activation volume for transformation in natural olivine is similarly low, and that direct conversion to the γ phase by the martensitic-like mechanism is possible at pressure conditions equivalent to the bottom of the transition zone. These observations have important consequences for models of subducting slabs and indicate that further study of the kinetics of martensitic-like transformation is warranted.

Acknowledgments

I thank A. Brearley, K. Leinenweber, I. Getting, D. Weidner, P. Heaney, and R. Reeder for helpful discussions as well as D. Rubie and W.A. Bassett for thoughtful reviews. The high-pressure experiments reported in this paper were performed in the Stony Brook High Pressure Laboratory, which is jointly supported by the National Science Foundation Science and Technology Center for High Pressure Research (EAR-8920239) and the State University of New York. Other research costs were supported by the Center for High Pressure Research at both Princeton University and the State University of New York at Stony Brook. MPI Publication no. 155.

References cited

Akaogi, M., Ito, E., and Navrotsky, A. (1989) Olivine-modified spinel-spinel transitions in the system Mg_2SiO_4-Fe_2SiO_4: Calorimetric measurements, thermochemical calculations, and geophyscial applications. Journal of Geophysical Research, 94, 15671–15685.

Boland, J.M., and Liu, L. (1983) Olivine to spinel transformation in Mg_2SiO_4 via faulted structures. Nature, 303, 233–235.

Burnley, P.C. (1990) The effect of nonhydrostatic stress on the olivine-spinel transformation in Mg_2GeO_4, 187 p. Ph.D. thesis, University of California, Davis, California.

Burnley, P.C., and Green, H.W., II (1989) Stress dependence of the mechanism of the olivine-spinel transformation. Nature, 338, 753–756.

Burnley, P.C., Green, H.W., II, and Prior, D.J. (1991) Faulting associated with the olivine to spinel transformation in Mg_2GeO_4 and its implications for deep-focus earthquakes. Journal of Geophysical Research, 96, 425–443.

Burnley, P.C., Bassett, W.A., and Wu, T.-c. (1995) The effect of large differential stresses and resultant strains on reconstructive transformation from the olivine to spinel phase in Co_2SiO_4, Ni_2SiO_4 and Mg_2GeO_4. Journal of Geophysical Research, 100, 17715–17724.

Christian, J.W. (1975) Transformation in metals and alloys: I. Equilibrium and general kinetic theory, 586 p. Pergamon, Oxford, U.K.

Dachille, F., and Roy, R. (1960) High pressure studies of the system, Mg_2GeO_4-Mg_2SiO_4 with special reference to the olivine-spinel transition. American Journal of Science, 258, 225–246.

Furnish, M.D., and Bassett, W.A. (1983) Investigation of the mechanism of the olivine-spinel transition in fayalite by synchrotron radiation. Journal of Geophysical Research, 88, 10333–10341.

Green, H.W., and Burnley, P.C. (1989) A new self-organizing mechanism for deep-focus earthquakes. Nature, 341, 733–737.

Green, H.W., Young, T.E., Walker, D., and Scholz, C.H. (1990) Anticrack-associated faulting at very high pressure in natural olivine. Nature, 348(6303), 720–722.

Gwanmesia, G.D., and Liebermann, R.C. (1992) Polycrystals of high-pressure phases of mantle minerals: Hot-pressing and characterization of physical properties. In Y. Syono and M.H. Manghnani, Eds., High-pressure research: Application to earth and planetary sciences, p. 117–135. American Geophysical Union, Washington, DC.

Iidaka, T., and Suetsugu, D. (1992) Seismological evidence for metastable olivine inside a subducting slab. Nature, 356, 593–595.

Kirby, S.H. (1987) Localized polymorphic phase transformation in high-pressure faults and applications to the physical mechanism of deep focus earthquakes. Journal of Geophysical Research, 92, 13789–13800.

Kirby, S.H., Durham, W.B., and Stern, L.A. (1991) Mantle phase changes and deep-earthquake faulting in subducting lithosphere. Science, 252, 216–225.

Kumazawa, M., and Anderson, O.L. (1969) Elastic moduli, pressure derivatives and temperature derivatives of single-crystal olivine and single-crystal forsterite. Journal of Geophysical Research, 74, 5961–5972.

Lacam, A., Madon, M., and Poirier, J.P. (1980) Olivine glass and spinel formed in a laser heated diamond-anvil high pressure cell. Nature, 228, 155–157.

Liebermann, R.C., and Wang, Y. (1992) Characterization of sample environment in a uniaxial split-sphere apparatus. In Y. Syono and M.H. Manghnani, Eds., High-pressure research: Application to earth and planetary sciences, p. 19–31. American Geophysical Union, Washington, DC.

Liu, L.G., and Bassett, W.A. (1986) Elements, oxides, and silicates high-pressure phases with implications for the Earth's interior, 250 p. Oxford University Press, New York.

Lomnitz-Adler, J. (1990) Are deep focus earthquakes caused by martensitic transformation? Journal of the Physics of the Earth, 38, 83–98.

Madon, M., Guyot, F., Peyronneau, J., and Poirier, J.P. (1989) Electron microscopy of high pressure phases synthesized from natural olivine in diamond anvil cell. Physics and Chemistry of Minerals, 16, 320–330.

Martinez, I., Wang, Y., Guyot, F., and Liebermann, R.C. (1994) Evolution of microstructures and iron partitioning in perovskite-magnesiowustite assemblages produced by disproportionation of San Carlos olivine. Eos, 75(44), 613.

Meade, C., and Jeanloz, R. (1989) Acoustic emissions and shear instabilities during phase transformations in Si and Ge and ultrahigh pressures. Nature, 339, 616–618.

Poirier, J.P. (1981) Martensitic olivine-spinel transformation and plasticity of the mantle transition zone. In American Geophysical Union Geodynamics Series, 4, 113–117.

——— (1991) Introduction to the physics of the Earth's interior, 264 p. Cambridge University Press, Cambridge, U.K.

Rigden, S.M., Gwanmesia, G.D., Fitz Gerald, J.D., Jackson, I., and Liebermann, R.C. (1991) Spinel elasticity and seismic structure of the transition zone of the mantle. Nature, 354, 143–145.

Ringwood, A.E. (1956) The system Mg_2SiO_4-Mg_2GeO_4. American Journal of Science, 254, 707–711.

Ross, N., and Navrotsky, A. (1987) The Mg_2GeO_4 olivine-spinel phase transformation. Physics and Chemistry of Minerals, 14, 473–481.

Rubie, D.C., and Champness, P.E. (1987) The evolution of microstructure during the transformation of Mg_2GeO_4 olivine to spinel. Bulletin de Minéralogie, 110, 471–480.

Rubie, D.C., and Ross, C.R., II. (1994) Kinetics of the olivine-spinel transformation in subducting lithosphere: Experimental constraints and implications for deep slab processes. Physics of the Earth and Planetary Interiors, 86, 223–241.

Rubie, D.C., Tsuchida, Y., Yagi, T., Utsumi, W., Kikegawa, T., Shimomura, O., and Brearley, A.J. (1990) An in-situ X ray diffraction study

of the kinetics of the Ni_2SiO_4 olivine spinel transformation. Journal of Geophysical Research, 95, 15829–15844.

Rubie, D.H. (1993) Mechanisms and kinetics of reconstructive phase transformations in the Earth's mantle. In Short Course Handbook on Experiments at High Pressure and Applications to the Earth's Mantle, 21, 247–303.

Sung, C.M. (1979) Kinetics of the olivine-spinel transition under high pressure and temperature: Experimental results and geophysical implications. In K.D. Timmerhaus and M.S. Barber, Eds., High-pressure science and technology, p. 31–41. Plenum, New York.

Sung, C.M., and Burns, R.G. (1976) Kinetics of high-pressure phase transformations: Implications to the evolution of the olivine-spinel transition in the down going lithosphere and its consequences to the dynamics of the mantle. Tectonophysics, 31, 1–32.

Vaughan, P.J., and Coe, R.S. (1981) Creep mechanism in Mg_2GeO_4: Effects of a phase transition. Journal of Geophysical Research, 86, 389–404.

Webb, S.L. (1989) The elasticity of the upper mantle orthosilicates olivine and garnet to 3 GPa. Physics and Chemistry of Minerals, 16, 684–692.

Weidner, D.J., and Hamaya, N. (1983) Elastic properties of the olivine and spinel polymorphs of Mg_2GeO_4, and evaluation of elastic analogues. Physics of the Earth and Planetary Interiors, 33, 275–283.

Weidner, D.J., Sawamoto, H., Sasaki, S., and Kumazawa, M. (1984) Single-crystal elastic properties of the spinel phase Mg_2SiO_4. Journal of Geophysical Research, 89, 7852–7860.

Wu, T.-c., Bassett, W.A., Burnley, P.C., and Weathers, M.S. (1993) Shear-promoted phase transformation in Fe_2SiO_4 and Mg_2SiO_4 and the mechanism of deep earthquakes. Journal of Geophysical Research, 98, 19767–19776.

Manuscript received February 6, 1995
Manuscript accepted July 17, 1995